

# A MACHINE VISION SYSTEM FOR FORENSIC ANALYSIS

Ovidiu Ghita<sup>1</sup>, René Gapert<sup>2</sup>, Laura Monks<sup>1</sup>, Jason Last<sup>2</sup> and Paul F. Whelan<sup>1</sup>

<sup>1</sup>Vision Systems Group, School of Electronic Engineering  
Dublin City University, Dublin 9, Ireland  
Email: ghita@eeng.dcu.ie, laura.monks2@mail.dcu.ie, whelanp@eeng.dcu.ie

<sup>2</sup>Forensic Anthropology Unit, Department of Human Anatomy and Physiology,  
University College Dublin, Earlsfort Terrace, Dublin 2, Ireland  
Email: rene.gapert@ucd.ie, jason.last@ucd.ie

## Abstract

Human skeletal remains are analysed by forensic anthropologists in order to draw conclusions about the probable identity of the deceased. During the analysis, the skull is used, along with other bones, to help determine the identity of the decedent. If only the base of the skull is available, forensic researchers take manual measurements from the large oval aperture in this region, the foramen magnum, in order to obtain information about the gender of the deceased. As this operation requires human intervention, the measurements are affected by the bias introduced by the human operator. The aim of this paper is to describe a full machine vision solution to perform precise morphological measurements of the foramen magnum. The system has been designed to extract measurements from 2D and 3D data and the returned results accurately match the manual measurements.

**Keywords:** Foramen magnum, semi-automatic segmentation, surface orientation, viewpoint rectification.

## 1. Introduction

The determination of gender for unidentified human remains is a key aspect for forensic anthropologists as this information can be used for legal investigations or the study of past populations [2,8,9]. In this regard, forensic anthropologists work in conjunction with homicide investigators in order to identify unique features (sex, age, ancestry, stature, etc.) of the deceased person from skeletal remains.

In forensic science, the skull is more frequently and thoroughly investigated than any other section of the human skeleton. In this paper, part of the adult skull known as the occipital bone will be used to obtain information that can be used to establish the gender of the deceased. It is worth noting that the human skull is a complex structure and a large number of measurements and calculable indices can be performed in order to obtain identification details about the deceased person, but in cases where only the occipital bone is available, more research is required before drawing conclusion on the decedents profile. In this study, the occipital bone of the skull is of high interest as this bone segment is least affected by inhumation and other physical damages. Foramen magnum is a large oval aperture that pierces the occipital bone. This region of the skull has been examined in the past in order to find ethnic and gender discriminative measures [7,8,9]. Among the most important measurements are the length (LFM), width (WFM), circumference (FMC) and area (FMA) of the foramen magnum.

Currently, the LFM and WFM parameters are measured using callipers and the FMC is measured by pressing a strip of paper around the edge of the foramen magnum, and the indentations left on the paper are measured to estimate this parameter. As these measurements are affected by the bias introduced by the human operator a vision system may offer a more robust approach for attaining these parameters.

In this paper we describe the implementation of a vision system based on intelligent scissors that can be successfully employed to extract the foramen magnum in 2D and 3D data and algorithmically measure the WFM, LFM, FMC. Also the system is able to provide information about the area and morphology of the foramen magnum. Our experiments have indicated that automated measurements for LFM and WFM closely match the manual measurements. The experimental results for FMC and foramen magnum area (FMA) indicate that the method employed to estimate these parameters manually provides inaccurate results especially in cases when the foramen magnum presents a complex shape. The forensic anthropologists utilise a number of empirical formulas to estimate the area of the foramen magnum that are not capable of offering a precise measurement when the foramen magnum presents complex shapes [7]. The developed system measures the actual area enclosed by the foramen magnum's outline and it is important to mention that the devised system offers real-time operation. The paper is organised as follows. Section 2 briefly introduces the semi-automatic intelligent scissors segmentation algorithm and the results obtained from 2D data are discussed. Section 3 presents the 3D viewpoint rectification algorithm and experimental results. Section 4 concludes this paper.

## 2. Image segmentation

The segmentation of foramen magnum from image data is challenging as often the skull is fragmented and the background is not well defined. Even in cases when the skull is complete, the imaged area of the foramen magnum is unevenly illuminated and this precludes the application of automatic techniques to identify the foramen magnum. In addition at the right and left of foramen magnum the occipital condyles are present and they may obstruct/overlap the outline of the foramen magnum (see Figure 1).

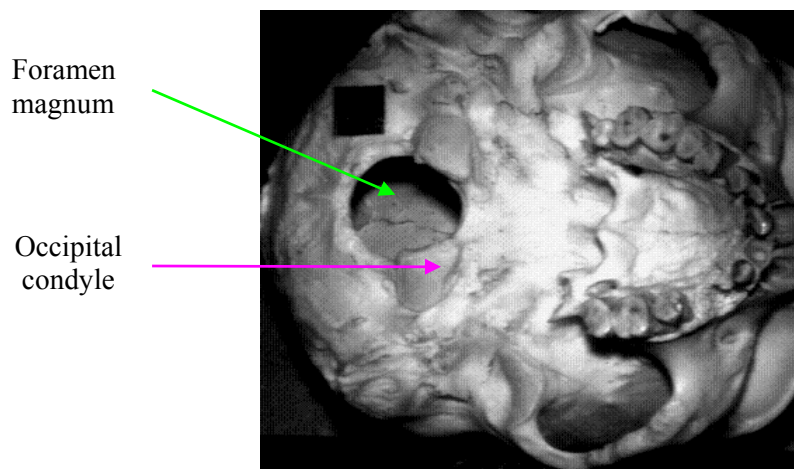


Figure 1. The base of the skull. It can be observed that the outline of the foramen magnum is obstructed by the occipital condyle. Also note the undesired effects caused by the uneven illumination and the cracks on the background bone.

These earlier mentioned challenges and the expert supervision required to perform accurate segmentation of the foramen magnum prompted us to implement a semi-automatic segmentation technique. As the outline of the foremen magnum is apparent we decided to use the gradient data to assist the segmentation. To this end, we implemented a version of the intelligent scissors algorithm that has been initially developed by Mortensen and Barrett [6]. This algorithm extracts the high gradient information contained in the image and the user has to select only an initial seed point placed close to the contour of the foramen magnum. Then, by moving the mouse cursor close to the contour of the foramen magnum, the algorithm will select the optimal path between the position of the mouse cursor and the seed point by snapping a curve to the highest gradient position, see Figure 2.

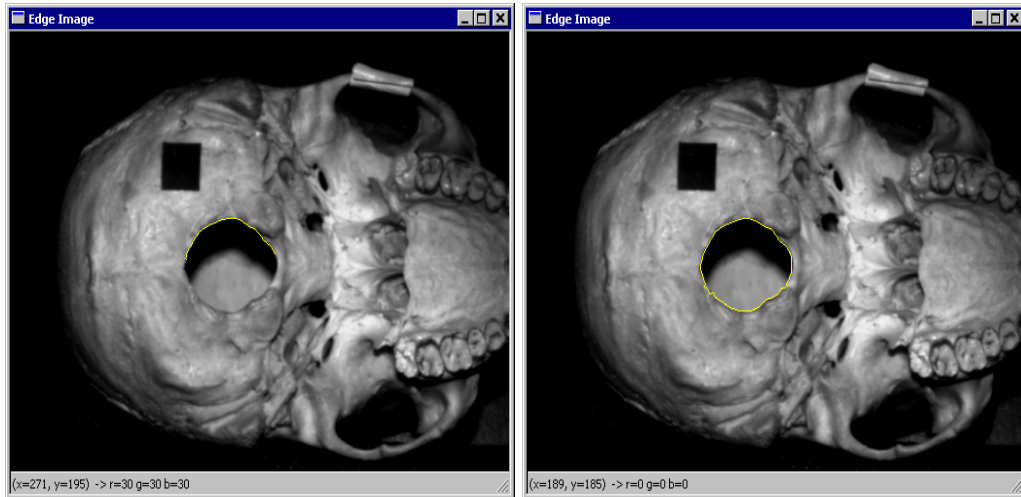


Figure 2. Intelligent scissors segmentation. The algorithm automatically stops when the segmented curve is closed (see right image).

If ambiguities are observed in the gradient data (i.e. the curve snaps to erroneous gradient points) the user can override the detected contour by inserting additional seed points by pressing the left mouse button. Once the contour of the foramen magnum has been completed (i.e. the extracted curve is closed) the algorithm identifies the area enclosed by the extracted contour and it will be used for detailed measurements. It is important to note, that although the user assists the segmentation process, the extracted curve is obtained by searching the optimal path in the gradient data and as a result the repeatability is excellent (for more details refer to Tables 1 and 2 where the repeatability has been evaluated for 10 successive trials).

The original algorithm developed by Mortensen and Barrett [6] determine the optimal path by performing a 2D dynamic programming graph search and in our implementation we replaced the zero-crossing edge detector with the more robust Canny edge detector [1]. This considerably reduced the situations when the intelligent scissors snapped to erroneous gradient data. Typical segmentation results are illustrated in Figure 3 where the LFM and WFM are over-imposed on the segmented area.

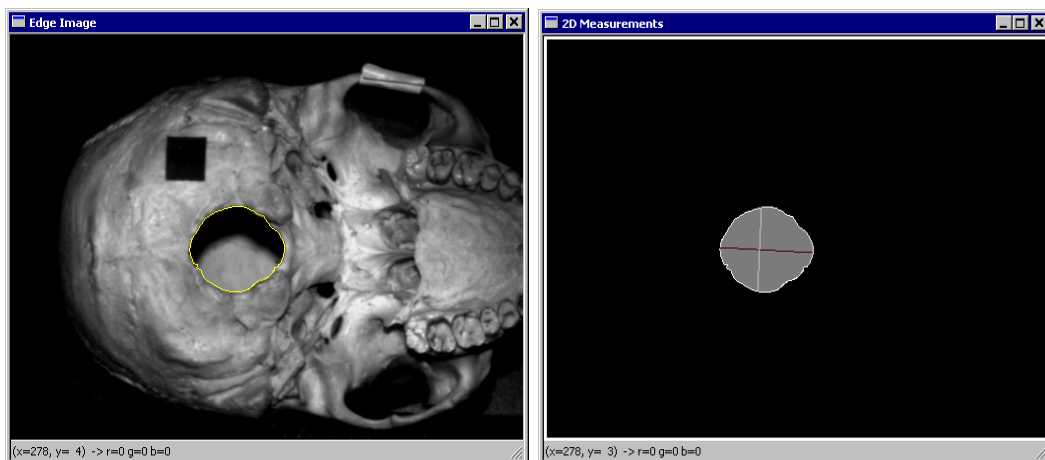


Figure 3. Segmentation results. (Left) Outline using the intelligent scissors. (Right) Segmented area with the LFM, WFM and FMC shown on the segmented data.

TRIALS	LFM (mm)	WFM (mm)
1	34.58	26.92
2	34.21	26.92
3	34.21	26.22
4	34.33	26.57
5	34.21	26.32
6	34.58	26.57
7	34.58	26.22
8	34.21	26.87
9	34.21	26.87
10	34.58	26.57
<b>Mean ± SD</b>	<b>34.37 ±0.18</b>	<b>26.65 ± 0.25</b>

Table 1. Repeatability tests on test skull 1. The mean value for LFM is 34.37 and the standard deviation is 0.18. For WFM the mean value is 26.65 and the standard deviation is 0.25.

TRIALS	LFM (mm)	WFM (mm)
1	37.21	33.56
2	37.33	33.91
3	37.21	33.56
4	37.21	33.91
5	37.21	33.91
6	37.21	33.56
7	36.94	33.56
8	37.21	33.91
9	36.94	33.56
10	37.21	33.91
<b>Mean ± SD</b>	<b>37.16 ±0.12</b>	<b>33.73 ± 0.18</b>

Table 2. Repeatability tests on test skull 2. The mean value for LFM is 37.16 and the standard deviation is 0.12. For WFM the mean value is 33.73 and the standard deviation is 0.18.

To calibrate the system a test object with known dimensions has been attached to the occipital bone to perform image calibration (see the dark square object illustrated in Figure 2). This object is used to identify the pixel dimension in  $x$  and  $y$  directions. The calibration object illustrated in Figure 2 is a square black rigid object where the length and width are 15mm. This calibration procedure is quite appropriate as it can be easily applied *in situ* where the skeletal remains are discovered.

The system can perform several measurements on the segmented region. The most important measurements are: the extraction of the width and length of the foramen magnum; calculate the foramen magnum circumference; calculate the estimated area using traditional empirical estimation formulas [8,9] and measure the actual area surrounded by the foramen magnum's contour. Also, the user can obtain several morphological measurements of the foramen magnum. In this regard, the user can obtain a measurement error when fitting the outline of the foramen magnum to an elliptical contour and also obtain the shape factor as the ratio between the minor and major axes of the fitted elliptical shape. These measurements can give a precise indication whether the shape of the foramen magnum is circular, elliptical or irregular.

The performance of the devised machine vision solution was evaluated by cross correlating the results obtained by the semi-automatic technique and the manual measurements obtained by the

Forensic Anthropology Unit in University College Dublin (UCD) [2]. For this purpose, we have selected 5 skulls (labelled as skull 6, 9, 11, 13 and 14) and the results for LFM, WFM and FMA obtained by the developed system are compared with those obtained by manual measurements. In addition we have included the actual area of the foramen magnum that is measured by the system. This measurement has not been measured manually as it was just approximated with empirical mathematical formulas. The numerical results obtained from this investigation are depicted in Table 3. In Table 3 the LFM and WFM are measured directly from segmented data, and the estimated area is obtained using 2 empirical formulas (circular approximation and using Texeira [9] approximation,  $\text{Area Texeira} = \pi \times [(h+w)/4]^2$ , where  $h$  and  $w$  are the measured height and width of the foramen magnum respectively). Actual area is obtained by multiplying the number of pixels contained in the segmented data with the pixel dimension obtained by calibration.

Skull index	LFM (mm)	WFM (mm)	Area Estimated Circular (mm <sup>2</sup> )	Area Estimated Texeira (mm <sup>2</sup> )	Actual Area (mm <sup>2</sup> )
<b>Skull 6</b>					
Manual	33.41	26.13	588.85	696.06	
Automated	34.35	26.74	576.94	732.77	702.10
<b>Skull 9</b>					
Manual	34.43	30.43	729.57	826.01	
Automated	35.89	31.32	701.55	886.94	870.98
<b>Skull 11</b>					
Manual	35.72	33.93	872.16	952.52	
Automated	36.41	34.45	817.46	985.89	990.75
<b>Skull 13</b>					
Manual	36.07	30.63	775.85	873.54	
Automated	36.15	31.56	736.57	900.19	852.65
<b>Skull 14</b>					
Manual	36.48	28.95	683.02	840.59	
Automated	36.66	29.15	652.47	850.38	799.36

Table 3. Automated and manual results. Note the difference between the empirically estimated area and measured area.

### 3. Measurements on 3D data

The measurements for LFM, WFM and FMA are precise only if the occipital bone is positioned so that the plane of the foramen magnum lies perpendicular to the optical axis of the camera (i.e. direction the camera points at the surface of interest). Otherwise the measurements are affected by the viewpoint distortions and the errors in measurement are in direct relation to the deviation angle. It is worth noting that the skull has a complex elongated shape and the procedure to position the optical axis of the camera perpendicular on the planar defined by the foramen magnum is time consuming and cumbersome. In fact the measurements will always be affected by the viewpoint distortions as the camera is positioned based only on observation. The viewpoint distortions can be eliminated if 3D data is available. In this regard, using the 3D data, the pose of the planar describing the foramen magnum with respect to the optical axis of the camera can be estimated. Then, by applying an orthographic projection the planar defined by the foramen magnum is forced to lie perpendicular to the direction of the optical axis of the camera. The steps outlined above will be detailed in the remainder of this section.

The first step consists of extraction of the 3D information of the base of the skull. For this purpose we employed the active depth from defocus (DFD) ranging technique to extract the depth information [3]. The active DFD range sensor is simple and involves a standard camera and a light projector that impose an artificial texture on the imaged object. The textural information supplied by the light projector is organised in equally spaced lines. The depth information is obtained by measuring the apparent blurring of the projected pattern [3,4].

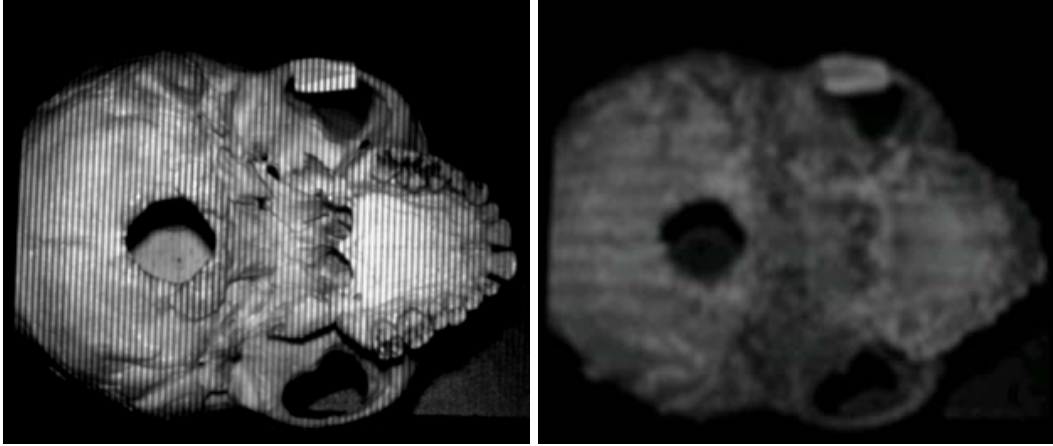


Figure 6. Actively illuminated skull and the computed range data. The objects placed closer to the camera have higher greyscale values in the range data.

Once the 3D data is computed using the abovementioned DFD range sensor, the next step is to estimate the position of the planar defined by the foramen magnum with respect to the optical axis of the camera (viewing direction). To do this we need to extract the range values of the points situated on the boundary of the foramen magnum (which are the points determined by the intelligent scissors algorithm). As we know that the 3D points associated with the outline of the foramen magnum (points determined by the intelligent scissors algorithm) lie on an approximately planar surface, the normal vector can be locally computed using the assumption that the elevation ( $z$  co-ordinate) is functionally dependent on the  $x$  and  $y$  co-ordinates. Thus, given a set of  $n$  points  $Q = [x, y, z]^T = [x_1 \dots x_n, y_1 \dots y_n, z_1 \dots z_n]$  from the range data that belong to the outline of the foramen magnum, the normal vector can be statistically computed by a planar fitting of the 3D points. The equation for a planar surface is  $z = a_1x + a_2y + a_3$  and the best fit can be determined in the least square sense [4] by minimising the errors between the  $z_i$  and the plane's values  $a_1x_i + a_2y_i + a_3$  as follows:

$$Err(\hat{a}) = \sum_{i=1}^n (\hat{a}_1x_i + \hat{a}_2y_i + \hat{a}_3 - z_i)^2 \quad (1)$$

where  $\hat{a} = [\hat{a}_1, \hat{a}_2, \hat{a}_3]$  are the estimated values. Eq. 1 generates a simultaneous system where the unknown values are  $\hat{a}$ . The normal vector calculated for surface  $Q = [x, y, z]^T$  can be represented in homogenous form as  $N = [n_x, n_y, n_z, 1]^T = [\hat{a}_1, \hat{a}_2, -1, 1]^T$ . Our aim is to obtain the transformation that projects the estimated planar of the surface  $Q = [x, y, z]^T$  onto the surface that is perpendicular on the optical axis of the camera (i.e. the normal vector lies along the  $z$  direction). Within the orthographic projection assumption [4], the image of the transformed plane can be simply formed by ignoring the  $z$  component of the transformed points (see Figure 7).

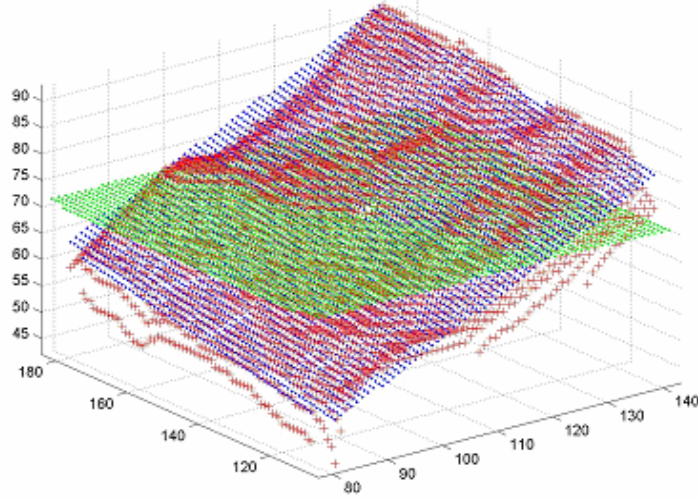


Figure 7. Orthographic projection. In red are the 3D points that define the surface  $Q = [x, y, z]^T$ , in blue is the least square estimated planar for  $Q$  surface and in green is the transformed planar (normal vector lies along z axis).

The desired transformation is formulated as  $H = T_0^{-1}R_yR_xT_0$  where  $T_0$  is a transformation that centres the points  $Q$  about the origin and  $R_x$  and  $R_y$  are the rotations about  $x$  and  $y$  axes.  $T_0$  has the form  $[I-M]$ , where  $M = [m_x, m_y, m_z, 1]^T$  is the mean vector  $M = \frac{1}{n} \sum_{i=1}^n P_i$  and  $I$  is the identity matrix. Rotations  $R_x$  and  $R_y$  have the following form:

$$R_x = \begin{bmatrix} 1 & 0 & 0 & 0 \\ 0 & \cos A_x & -\sin A_x & 0 \\ 0 & \sin A_x & \cos A_x & 0 \\ 0 & 0 & 0 & 1 \end{bmatrix} \quad R_y = \begin{bmatrix} \cos A_y & 0 & \sin A_y & 0 \\ 0 & 1 & 0 & 0 \\ -\sin A_y & 0 & \cos A_y & 0 \\ 0 & 0 & 0 & 1 \end{bmatrix} \quad (2)$$

where  $A_x = \tan^{-1}(n_y, n_z)$ . The rotation angle about  $y$  is computed using the transform  $N_{R_x} = R_x N = [n_{rx}, n_{ry}, n_{rz}, 1]^T$  and  $A_y = -\tan^{-1}(n_{rx}, n_{rz})$ .

In Eq. 2  $\tan^{-1}$  represents the four quadrant inverse tangent. Figure 8 depicts the result of this transformation when the detected angles between the normal of the foramen magnum and the camera's optical axis are  $-30.79^\circ$  about  $x$  axis and  $-21.10^\circ$  about  $y$  axis. The measurements obtained for LFM and WFM *before* orthogonal projection (skull 9) are 30.37mm, 26.82mm. We notice significant errors in estimation introduced by the viewpoint distortion. The results obtained for LFM and WFM *after* the orthographic projection is applied (skull 9) are 34.28mm and 28.52mm. From these results we can assess the efficacy of the orthographic projection described in this paper as these results compare well with those obtained when the camera was manually positioned in such way that its optical axis was perpendicular to the surface defined by foramen magnum (see Table 3). More precise results can be obtained if a range sensor with a higher resolution would be employed. The DFD range sensor used for this implementation has an accuracy of 3.4% of the overall ranging distance measured from the sensor [3]. Also, another inconvenience associated with this active ranging strategy is its inability to accurately measure the depth estimation when the sensor is applied to darkly coloured objects.



Figure 8. Segmented data. (Left) Before orthographic projection and (Right) after orthographic projection.

## 4. Conclusions

This paper details the implementation of a vision system that is able to extract the morphological measurements of the foramen magnum from 2D and 3D data. The current procedure to estimate the LFM, WFM and FMA involves a human operator driven method. As the measurements are manually obtained they are inherently subjected to intra and inter observer variability. Also some parameters such as FMC and FMA are only estimated using some empirical formulas [8,9] and actual results cannot be easily measured. In this paper we have described a vision system that is able to produce repeatable and accurate results in real time. In addition the operator can obtain information about the morphological structure of the foramen magnum and this may also prove useful in defining gender differences in human skulls, when applied to documented osteological collections.

## References

- [1] J. Canny, "A computational approach to edge detection", *IEEE Transactions on Pattern Analysis and Machine Intelligence*, 8(6), pp. 679-698, 1986.
- [2] R. Gapert and J. Last, "The adult human occipital bone: measurement variance and observer error", *Proceedings of the Fifth Annual Conference of the British Association for Biological Anthropology and Osteoarchaeology*, 2005.
- [3] O. Ghita and P.F. Whelan, "A video-rate sensor based on depth from defocus", *Optics & Laser Technology*, 33(3), pp. 167-176, 2001.
- [4] O. Ghita and P.F. Whelan, "A bin picking system based on depth from defocus", *Machine Vision and Applications* 13(4), pp. 234-244, 2003.
- [5] P. Lancaster and K. Salkauskas, "Curve and surface fitting: An introduction", London: Academic Press, 1986.
- [6] E.N. Mortensen and W.A. Barrett, "Interactive segmentation with intelligent scissors", *Graphical Models and Image Processing*, 5(60), pp. 349-384, 1998.
- [7] K.A. Murshed, A.E. Cicekcibasi and I. Tuncer, "Morphometric evaluation of the foramen magnum and variations in its shape: A study on computerized tomographic images of normal adults", *Turkish Journal of Medical Sciences*, 33, pp. 301-306, 2003.
- [8] R.V. Routal, G.P. Pal and S. Bhagawat, "Metrical studies with sexual dimorphism in foramen magnum of human crania", *Journal of Anatomical Society of India*, 33, pp. 85-89, 1984.
- [9] W.R.G. Teixeira, "Sex Identification utilizing the size of the foramen magnum", *American Journal of Forensic Medicine and Pathology*, 3(3), pp. 203-206, 1982.